

## Statistical error for cosmic ray modulation evaluation by a 1D model

---

Viacheslav Mykhailenko<sup>a</sup> and Pavol Bobík<sup>b</sup>

<sup>a</sup>*Institute of Physics, Faculty of Science, P. J. Safarik University,  
Park Angelinum 9, 041 54 Košice, Slovakia*

<sup>b</sup>*Institute of Experimental Physics, Slovak Academy of Sciences,  
Watsonova 47, Košice, Slovakia*

*E-mail: [viacheslav.mykhailenko@student.upjs.sk](mailto:viacheslav.mykhailenko@student.upjs.sk), [bobik@saske.sk](mailto:bobik@saske.sk)*

The propagation of cosmic rays through the heliosphere is solved for more than half a century by stochastic methods based on Ito's lemma. This work estimates the statistical error of the solution of the Fokker–Planck equation by a 1D forward stochastic differential equations method. The dependence of the error on simulation statistics and energy is presented for different combinations of input parameters. The 1% precision criterion in intensities and 1% criterion in standard deviation are defined as a function of the solar wind's velocity and the diffusion coefficient value.

*37<sup>th</sup> International Cosmic Ray Conference (ICRC 2021)  
July 12th – 23rd, 2021  
Online – Berlin, Germany*

## 1. Introduction

The Sun produces and radiates out a charged particle flow, which is called the solar wind. The solar wind propagates through the solar system and continues to the moment when the solar wind and the interstellar wind pressure are balanced. This spherical region, which has a radius that is equal approximately 100 AU, is called the heliosphere. The so-called solar modulation process begins when the galactic cosmic rays (GCRs) reach the heliosphere's boundary, which presents a decrease of GCR intensity inside the heliosphere (mostly for particles with energies less than 30 GeV). At the time of solar modulation, GCR particles interact with magnetic irregularities in the solar wind. This process can be approximated as a diffusion combined with convection and adiabatic energy losses. As was described by some early authors, the particle starts randomly walking between these irregularities. These irregularities move with the velocity of the solar wind. Consequently, the GCR's intensity is strongly anticorrelated concerning solar activity, and is also influenced by the interplanetary magnetic field polarity and GCR particle sign. Parker [1] introduced a widely-used equation to describe GCR propagation inside the heliosphere. One of the most precise methods to solve this equation is the so-called stochastic integration method. Using this approach, we can evaluate the solution calculated as the associated set of stochastic differential equations (SDEs), "forward-in-time" or "backward-in-time". However, we only used the forward-in-time stochastic integration approach for all of the simulations that are presented in this article. In this approach, quasi-particle objects were injected at the heliosphere's boundary. They then move in the Sun's direction to the inner heliosphere. Both forward and backward approaches descend from the Kolmogorov forward and Kolmogorov backward equations, which is the reason why they have the same mathematical description.

In this paper, we evaluate the solution of the Parker equation using the forward-in-time stochastic integration approach. For the sake of clarity, this article has focused on the solution of the 1D Parker equation. The solutions that are presented were evaluated for different sets of input parameters. The injection energy range was taken to be from 0.001 GeV up to 100 GeV.

## 2. Model description

In 1965, Parker proposed a transport equation that describes the GCR distribution inside the heliosphere. The equation that describes the solar modulation and particle propagation process in the heliosphere can be written through an omnidirectional distribution function  $f(\vec{x}, p)$ , with particle momentum  $p$  in the following form:

$$\frac{\partial f}{\partial t} = -\nabla \cdot (f\vec{V}) + \nabla \cdot [\vec{K} \cdot \nabla f] + \frac{\nabla \cdot \vec{V}}{3p^2} \frac{\partial}{\partial p} (p^3 f) \quad (1)$$

Here  $V = V_{sw} + V_{drift}$ ,  $V_{sw}$  is solar wind velocity,  $V_{drift}$  is the particle magnetic drift velocity,  $\vec{x}$  is the 3-D spatial position in Cartesian coordinates, and  $\vec{K}$  is the diffusion tensor. The differential intensity  $J$  is related to  $f$  as  $J = p^2 f$ .

The stochastic SDE set integrations should be performed in a Euclidean space. The set of the spatial position could be pronounced as a set of Cartesian coordinates [2]. In 2010, Pei et al. found that spherical coordinates can be successfully applied [3]. For 1D representation of the heliosphere

in spherical coordinates, and for the case where all parameters depend only on radius and energy, the Parker equations can be simplified to the following form [4][5]:

$$\frac{\partial f}{\partial t} = \frac{1}{r^2} \frac{\partial}{\partial r} \left( r^2 K \frac{\partial f}{\partial r} \right) - \frac{1}{r^2} \frac{\partial r^2 V f}{\partial r} + \frac{1}{3} \left( \frac{1}{r^2} \frac{\partial r^2 V}{\partial r} \right) \frac{1}{p^2} \frac{\partial}{\partial p} (p^3 f) \quad (2)$$

Where the diffusion tensor  $\tilde{K}$  was simplified to be a scalar  $K = K_0 \beta P$ , here  $K_0$  is the diffusion parameter,  $\beta$  is the particle velocity in speed of light units, and  $P$  is the rigidity in gigavolt units. Given that the magnetic field is assumed to be spherically symmetrical, the magnetic drift velocity in the radial direction is equal to zero.

### 3. Forward-in-time stochastic integrations

The time step for all of the forward-in-time stochastic integrations that are presented in this article is constant and taken to be  $\Delta t = 50s$ . The stochastic path of a particle in the forward-in-time approach is described by SDE (12)(13) and (14) in [5]. In this approach, a quasi-particle injected at the heliosphere's border (for all of the simulations presented in this work) is spherical with a radius of 100 AU and it does not have any structure (i.e., termination shock, heliosheath, heliopause, or bow shock). For each step of time, the particle lost its energy (momentum) by the value calculated in equation (13). Every time that the particle crosses a 1 AU registration radius, its actual energy and position are registered to an appropriated energy bin. The position at 0.01 AU was set as an inner reflecting boundary in all of the presented simulations (so-called mirroring). As pointed out by Pei et al. (2010), the quasi-particle object is not a real particle but is simply a point in phase space.

### 4. Spectra at 1AU from the SDE solution of FPE

The modulated spectra at 1 AU position were evaluated using the procedure described in [5] with LIS from [4], and thus the differential intensity was taken to be  $J \propto p(m^2 c^4 + p^2 c^2)^{-1.85}$ . In the presented simulations, the 1 AU position is taken to be a target because most of the measurements of the GCR inside the heliosphere were done at the Earth or in its orbit. The stochastic integration procedures were done for a different set of input parameters. For diffusion parameter  $K_0 = 3, 5, 7 \times 10^{22} cm^2 s^{-1} GV^{-1}$ , and the solar wind velocity  $V_{sw} = 300, 400, 500 km s^{-1}$ . For the data processing, we used the spectra with a linear energy bin size equal to 0.1 GeV. The modulated spectrum at 1AU that is shown in Figure 1 was evaluated for all of the sets of input parameters.

A presented spectrum is obtained for the whole injection energy range of each simulation. The one separate simulation is for 100000 particles injected at the heliosphere's border. Each particle was injected with an injection energy in a range from 0.001 GeV to 100 GeV, and the injection energy step is 0.001 GeV. Thus, in one so-called simulation, we have different injection energies for every injected particle. In Figure 1, it can be seen that the spectrum for diffusion parameter  $K_0 = 5 \times 10^{22} cm^2 s^{-1} GV^{-1}$ , and solar wind velocity  $V_{sw} = 400 km s^{-1}$  has a larger intensity with respect to other spectra because of the higher statistic (just about three million injected simulations; i.e.,  $300 \times 10^9$  injected particles) concerning other parameters sets (three hundred thousand injected simulations; i.e.,  $30 \times 10^9$  particles).

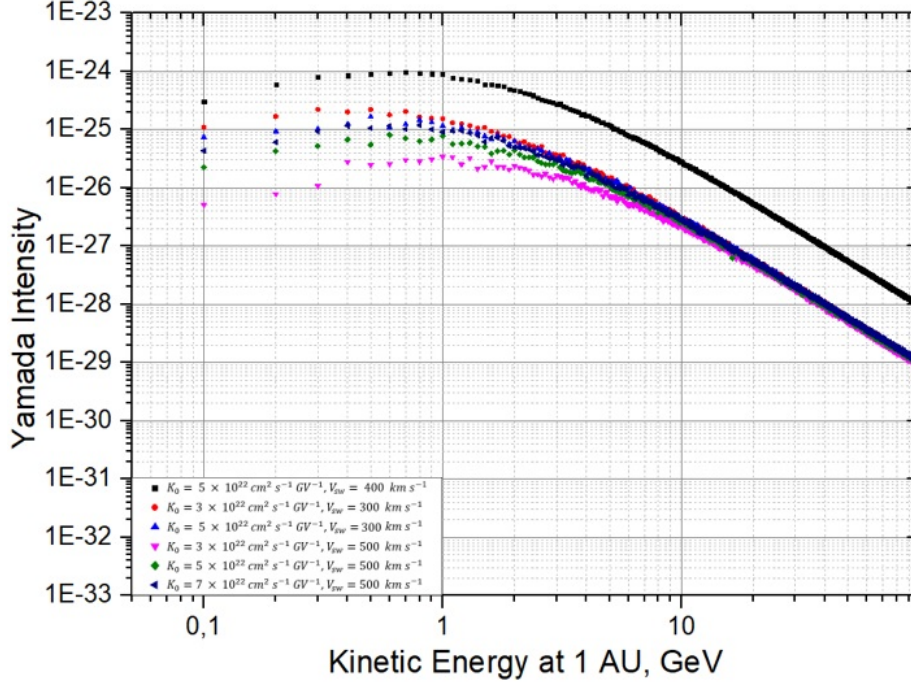


**Figure 1:** Local interstellar spectra at 1 AU evaluated for different sets of input parameters (for more details, see the text).

## 5. SDE method statistical error estimation

### 5.1 Statistical error for full spectrum at 1AU

To show the dependency of the statistical error on the number of injected particles, we first evaluated the dependency of the spectrum integral between energies 0.001 and 100 GeV at a number of simulations. We calculate the integrals of the whole energy spectra with respect to different numbers of simulations (Fig. 2). For example, for  $N=1000$ , we use for evaluation of modulated spectrum intensity one thousand simulations (i.e., one hundred million particles). We realise many such simulations with one hundred million particles (300 points) and every one of them is represented by a point at vertical line cross the  $N=1000$ . The obtained integral values were normalised by the number of simulations (by statistics) and then by the value of the integral evaluated for highest statistics. The 1 percent statistical error value is related to the value of this integral (i.e., the one with the highest statistics). Consequently, the integrals as a function of statistics for different sets of input parameters were evaluated.

Every separate integral value represents the sum of differential intensities at 1AU for the number of injected simulations. Therefore, it is possible to see that statistics is an important part in the solution of the Parker equation using the forward-in-time stochastic integration approach. The normalised integral value distribution converges to plus-minus one percent criterion for approximately three hundred thousand simulations. Most of the points lie close to reference case simulation with the highest statistics and they are inside the plus-minus one percent statistical error criterion border lines.

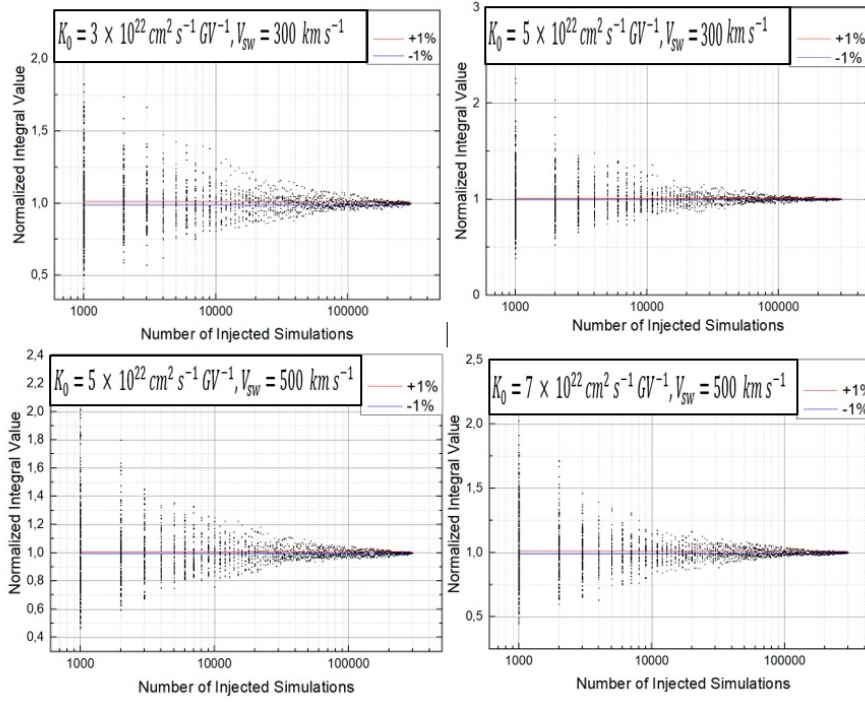


**Figure 2:** Normalised integrals distribution with respect to number of injected trajectories for different sets of input parameters ( $K_0 = 3 \times 10^{22} \text{ cm}^2 \text{ s}^{-1} \text{ GV}^{-1}$ ,  $V_{sw} = 300 \text{ km s}^{-1}$ ) top left-hand panel, ( $K_0 = 5 \times 10^{22} \text{ cm}^2 \text{ s}^{-1} \text{ GV}^{-1}$ ,  $V_{sw} = 300 \text{ km s}^{-1}$ ), top right-hand panel ( $K_0 = 5 \times 10^{22} \text{ cm}^2 \text{ s}^{-1} \text{ GV}^{-1}$ ,  $V_{sw} = 500 \text{ km s}^{-1}$ ), bottom left-hand panel, and ( $K_0 = 7 \times 10^{22} \text{ cm}^2 \text{ s}^{-1} \text{ GV}^{-1}$ ,  $V_{sw} = 500 \text{ km s}^{-1}$ ) bottom right-hand panel

For a better understanding of the dependency of the statistical error on the input parameters, the standard deviation of distribution concerning the number of injected simulations was obtained from the presented integrals. For every  $N$ , we evaluated the standard deviation of all available normalised integral values (see Fig. 3).

Figure 3 shows that the standard deviation for results with a number of simulations  $N = 10000$  is close to 0.1. From the figure, we can see that we need more than  $N = 100000$  simulations to reach a standard deviation of 0.01 in the integral values of the whole spectrum. The standard deviation depends on  $N$  with power-law shape, except for the cut off at the end with high  $N$  values. For the largest evaluated statistics case, the standard deviation value is around 0.0001. For some sets of parameters, it will be smaller than for other sets. However, the low statistics are the reason for cut-off tail shape at the high statistics. The standard deviation is only evaluated from a few spectra integrals.

Finally, we obtained linear fits from the standard deviation distribution in the range from 1000 to 10000 injected simulations (Fig. 4). This range was taken because standard deviations in this range are evaluated from biggest number of integrals. Consequently, points in this range have in the logarithmic scale a smooth linear slope (power law shape) and therefore it is possible to evaluate linear fit.

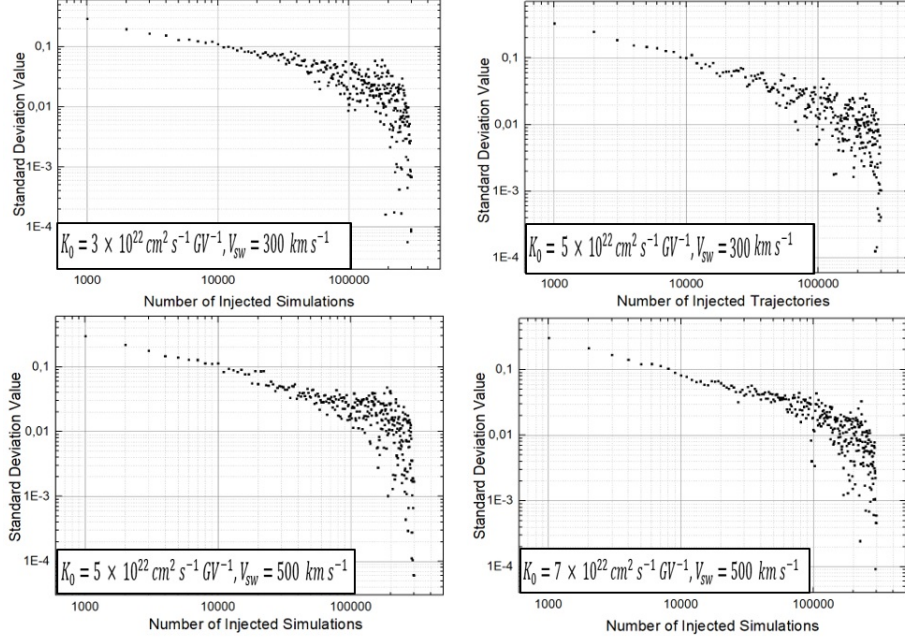


**Figure 3:** Standard deviation evaluated from normalised integrals ( $K_0 = 3 \times 10^{22} \text{cm}^2 \text{s}^{-1} \text{GV}^{-1}$ ,  $V_{sw} = 300 \text{km s}^{-1}$ ) top left-hand panel, ( $K_0 = 5 \times 10^{22} \text{cm}^2 \text{s}^{-1} \text{GV}^{-1}$ ,  $V_{sw} = 300 \text{km s}^{-1}$ ), top right-hand panel ( $K_0 = 5 \times 10^{22} \text{cm}^2 \text{s}^{-1} \text{GV}^{-1}$ ,  $V_{sw} = 500 \text{km s}^{-1}$ ), bottom left-hand panel, and ( $K_0 = 7 \times 10^{22} \text{cm}^2 \text{s}^{-1} \text{GV}^{-1}$ ,  $V_{sw} = 500 \text{km s}^{-1}$ ) bottom right-hand panel

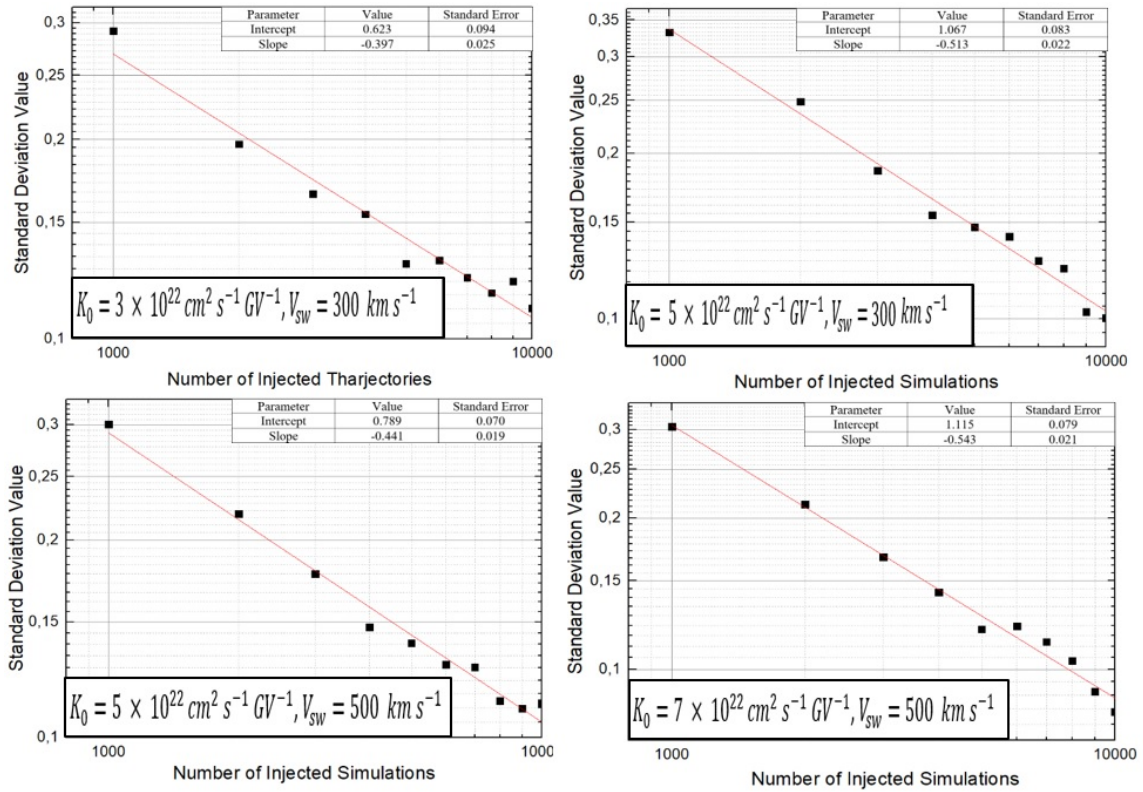
The standard deviation for 10 thousand simulations obtained from fits in the range between 1000 and 10000 simulations is presented in Table 1. The results show that STD from 10 thousand simulations varies for the used range of input parameters between 0.082 and 0.129.

Assuming that the power law dependency fitted in a range from 1000 to 10000 simulations could be extended to higher values of  $N$ , we could find a number of simulations needed to reach standard deviation 0.01 of spectrum integral noted as  $N_{0.01}$  (i.e., intensity of cosmic rays with STD value 0.01). The fits parameters for different combinations of input parameters (i.e., for solar wind velocity and diffusion parameter) are presented in Table 1. The  $N_{0.01}$  found for the combinations of input parameters that we used vary between six million for  $K_0 = 3 \times 10^{22} \text{cm}^2 \text{s}^{-1} \text{GV}^{-1}$ ,  $V_{sw} = 400 \text{km s}^{-1}$  and half a million for  $K_0 = 7 \times 10^{22} \text{cm}^2 \text{s}^{-1} \text{GV}^{-1}$ ,  $V_{sw} = 500 \text{km s}^{-1}$ . Generally, the standard deviation  $N_{0.01}$  decreases with higher values of the diffusion parameter. However, the dependency of  $N_{0.01}$  on solar wind speed is less clear.

In conclusion, to reach the standard deviation of spectrum integral at a level of 10 percent, we need to inject approximately one or a couple of billion particles into the heliosphere. To reach a standard deviation at a level of 1 percent, we need to inject approximately hundreds of billions of particles into the heliosphere.

We will extend the range of input parameters, specifically solar wind speed values, in our future research and we will apply the same methods shown here to selected energy bins, which will show the error estimation for different energy bins.

Input parameters	STD value at $10^4$ simulations	Slope	Intercept	$N_{0.01}$
$K_0 = 3 \times 10^{22} \text{cm}^2 \text{s}^{-1} \text{GV}^{-1}, V_{sw} = 300 \text{km s}^{-1}$	0,111	-0.397	0.623	4 046 251
$K_0 = 3 \times 10^{22} \text{cm}^2 \text{s}^{-1} \text{GV}^{-1}, V_{sw} = 400 \text{km s}^{-1}$	0,129	-0.444	0.836	2 439 986
$K_0 = 3 \times 10^{22} \text{cm}^2 \text{s}^{-1} \text{GV}^{-1}, V_{sw} = 500 \text{km s}^{-1}$	0,123	-0.390	0.645	6 054 123
$K_0 = 5 \times 10^{22} \text{cm}^2 \text{s}^{-1} \text{GV}^{-1}, V_{sw} = 300 \text{km s}^{-1}$	0,100	-0.513	1.067	951 825
$K_0 = 5 \times 10^{22} \text{cm}^2 \text{s}^{-1} \text{GV}^{-1}, V_{sw} = 400 \text{km s}^{-1}$	0,097	-0.493	0.943	932 339
$K_0 = 5 \times 10^{22} \text{cm}^2 \text{s}^{-1} \text{GV}^{-1}, V_{sw} = 500 \text{km s}^{-1}$	0,113	-0.441	0.789	2 109 905
$K_0 = 7 \times 10^{22} \text{cm}^2 \text{s}^{-1} \text{GV}^{-1}, V_{sw} = 300 \text{km s}^{-1}$	0,113	-0.477	0.954	1 559 093
$K_0 = 7 \times 10^{22} \text{cm}^2 \text{s}^{-1} \text{GV}^{-1}, V_{sw} = 400 \text{km s}^{-1}$	0,090	-0.504	0.970	781 370
$K_0 = 7 \times 10^{22} \text{cm}^2 \text{s}^{-1} \text{GV}^{-1}, V_{sw} = 500 \text{km s}^{-1}$	0,082	-0.543	1.115	545 316

**Table 1:** Fit parameters evaluated from linear fits in range from 1000 to 10000 injected simulations

**Figure 4:** Linear fit evaluated from standard deviation distribution in range from 1000 to 10000 simulations ( $K_0 = 3 \times 10^{22} \text{cm}^2 \text{s}^{-1} \text{GV}^{-1}, V_{sw} = 300 \text{km s}^{-1}$ ) top left-hand panel, ( $K_0 = 5 \times 10^{22} \text{cm}^2 \text{s}^{-1} \text{GV}^{-1}, V_{sw} = 300 \text{km s}^{-1}$ ) top right-hand panel ( $K_0 = 5 \times 10^{22} \text{cm}^2 \text{s}^{-1} \text{GV}^{-1}, V_{sw} = 500 \text{km s}^{-1}$ ), bottom left-hand panel, and ( $K_0 = 7 \times 10^{22} \text{cm}^2 \text{s}^{-1} \text{GV}^{-1}, V_{sw} = 500 \text{km s}^{-1}$ ) bottom right-hand panel

## 6. Conclusions

The cosmic ray spectra at 1 AU were evaluated in the F-p method for Yamada LIS spectra for the energy range from 0.001 to 100 GeV, for six sets of input parameters (see Fig. 1). The integrals for the whole energy range were evaluated to show the dependence of the statistical error on the number of injected simulations (see Fig. 2). The standard deviation distribution with respect to the number of injected simulations (see Fig. 3) was obtained from evaluated whole energy range normalised integrals. Linear fits of standard deviation in the range from 1000 to 10000 injected simulations were shown (see Fig 4). The fit parameters are presented in Table 1.

## 7. Acknowledgment

The Slovak VEGA grant agency, project 2/0077/20 is acknowledged, for the support.

## References

- [1] E. N. Parker. “The passage of energetic charged particles through interplanetary space”. In: 13.1 (Jan. 1965), pp. 9–49. doi:10.1016/0032-0633(65)90131-5.
- [2] Ming Zhang. “A Markov stochastic process theory of cosmic-ray modulation”. In: 513.1 (Mar. 1999), pp. 409–420. doi:10.1086/306857.
- [3] C. Pei et al. “A general time-dependent stochastic method for solving Parker’s transport equation in spherical coordinates”. In: *Journal of Geophysical Research (Space Physics)* 115.A12, A12107 (Dec. 2010), A12107. doi:10.1029/2010JA015721.
- [4] Yoshihiko Yamada, Shohei Yanagita, and Tatsuo Yoshida. “A stochastic view of the solar modulation phenomena of cosmic rays”. In: 25.13 (Jan. 1998), pp. 2353–2356. doi:10.1029/98GL51869.
- [5] P. Bobik et al. “On the forward-backward-in-time approach for Monte Carlo solution of Parker’s transport equation: One-dimensional case”. In: *Journal of Geophysical Research (Space Physics)* 121.5 (May 2016), pp. 3920–3930. doi:10.1002/2015JA022237.